Environmental Technology & Innovation 40 (2025) 104576

Contents lists available at ScienceDirect

Environmental Technology & Innovation

journal homepage: www.elsevier.com/locate/eti

# New insights on electrochemical remediation of soil/sediments: In situ phenol transformation and mineralization in spiked kaolin under low electric fields

Federica Proietto *, Vito Musacchia, Claudia Prestigiacomo, Alessandro Galia, Onofrio Scialdone

*Dipartimento di Ingegneria, Università degli Studi di Palermo, Viale delle Scienze, Ed. 6, Palermo 90128, Italy*

ARTICLE INFO

*Keywords:*
Electrochemical Remediation
ECGO
Low electric field
Sediments/Soils
Phenol
Carboxylic acids
$CO_2$

ABSTRACT

Most studies on electrochemical remediation of soil/sediment focus on the removal efficiency of one or more target organic contaminants without considering their evolution during the transformation and the possible release of other pollutants in the environment. In this study, the effect of electrochemical remediation (ER) of spiked kaolin on the transformation of phenol (PhOH) into many potential byproducts was investigated under very low electric fields (*E*). ER under 0.15 V $cm^{-1}$ was performed using cheap graphite electrodes in direct contact with the spiked kaolin with PhOH for 8, 24, 48, 96, 168 and 336 h. This study shows that the ER under low *E* value is an appropriate approach to concurrently desorb, mobilize and in-situ remove PhOH up to 70 % after 14 days, and for the first time, that PhOH in spiked kaolin is converted into several carboxylic acids (CAs), including maleic acid, formic acid and oxalic acids. They are simultaneously produced by PhOH oxidation and consumed by their following oxidation. Indeed, it was observed that the TOC/TOC° value decreases significantly to 38 ± 10 % after 14 days, thus showing that an appreciable content of PhOH is converted to $CO_2$ and water. This study points out that the ER process under very low *E* values might be an in situ viable way to oxidize hazardous organic contaminants into harmless compounds up to carbon dioxide and water without adding enhancing agents and at low energy consumption.

## 1. Introduction

One of the last decade's crucial priorities is environmental healthiness and agriculture preservation (EU, Soil Strategy for, 2023). In 2021, in the EU Soil Strategy for 2030 program agenda, the European Commission defined concrete actions by 2023 to remediate contaminated sites and restore soils to achieve healthy soils by 2050 (EU, Soil Strategy for, 2023). Remediation of contaminated soils/sediments is challenging since they are characterized by *i*) fine grains, *ii*) heterogeneous conditions, *iii*) low-hydraulic permeability, and *iv*) miscellaneous persistent inorganic and organic contaminants (Li and Li, 2025). These pollutants are polychlorinated biphenyl (PCB), polycyclic aromatic hydrocarbons (PAHs), hexachlorobenzene, total petroleum hydrocarbons (TPHs), phenolic compounds, heavy metals (i.e. Hg, As, Pb, Cr, Zn) and radionuclides. They are usually highly concentrated, and sites require imminent restoration. Phenolic compounds and, more in detail, phenol (PhOH) are distinctive toxic organic pollutants located in soil. They are

* Corresponding author.
*E-mail address:* federica.proietto@unipa.it (F. Proietto).

https://doi.org/10.1016/j.eti.2025.104576
Received 21 July 2025; Received in revised form 15 September 2025; Accepted 18 October 2025
Available online 19 October 2025

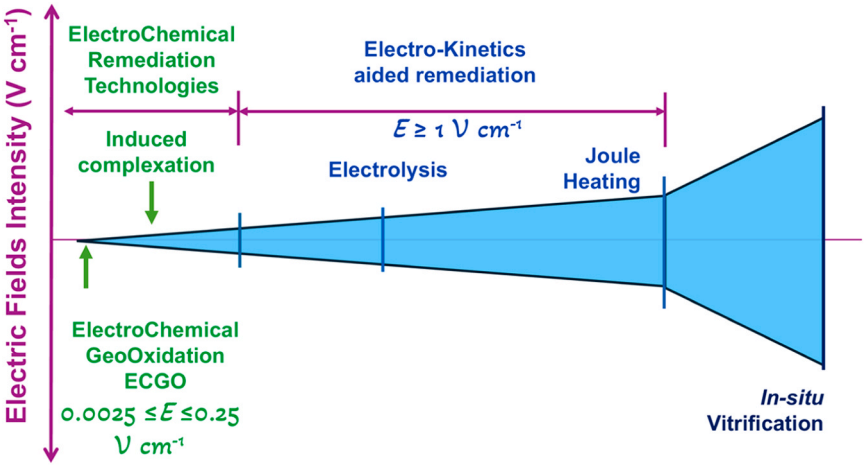


**Fig. 1.** Type of DCTs for remediation of soils and sediments as a function of the *E* intensity.

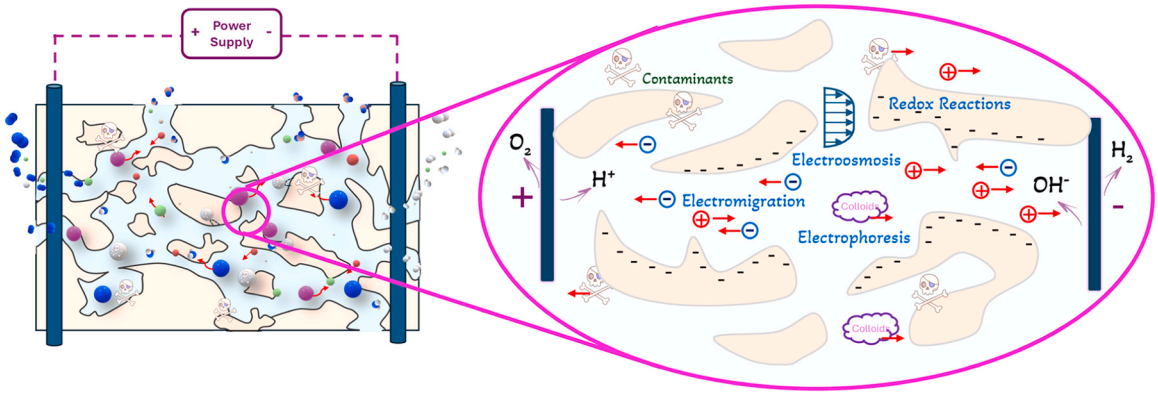


**Fig. 2.** Zoom area schematic view of the DTCs and the reaction mechanism in treating contaminated sites.

listed among the priority contaminants because they are hazardous to the ecosystem and human health, due to their toxicity and recalcitrant nature (Annamalai et al., 2022; Barati Fardin and Jamshidi-Zanjani, 2025; Cui et al., 2006; Thepsithar and Roberts, 2006). The conventional approaches to cleaning up these polluted sites include landfilling or incineration, which are expensive, disruptive and unsustainable (Gomes et al., 2013). Conversely, when dredging or related strategies are used for environmental issues, the main problem is only moved to other stages and not overcome (Amato et al., 2026, Perelo, 2010). Therefore, more cost-effective and less invasive technologies are necessary (Perelo, 2010). In this context, in-situ technologies allow remediation without removing soil/-sediment from the source sites but with unknown long-term effects (Libralato et al., 2018). In the last decade, thermal, electrochemical, ultrasonic, biological and physiochemical approaches have been investigated in detail (Annamalai et al., 2022; Li et al., 2017; Lofrano et al., 2017; Mouli et al., 2004; Ossai et al., 2020). Among these routes, Direct Current Technologies (DCTs) are regarded as among the *i*) most cost-effective, *ii*) sustainable, *iii*) environmentally friendly, *iv*) non-invasive and *v*) practical for both ex-situ and in-situ approaches regarding other investigated strategies (Barati Fardin and Jamshidi-Zanjani, 2025; Proietto et al., 2023). DCTs are based on electrochemical principles. During these treatments, a direct current passes through the wet soil/sediment by applying a cell potential between electrodes placed in direct contact or nearby to the polluted site, inducing an electric field to it ($E$ [=] V cm$^{-1}$). DCTs are classified into ElectroChemical Remediation Technologies (ECRTs $E <$ 1 cm$^{-1}$) and ElectroKinetics (EKs $E \geq$ 1 cm$^{-1}$) (Fig. 1) (McIlvride et al., 2003). ECRTs include induced complexation (which complexes metal pollutants) and ElectroChemical GeoOxidation (ECGO; 0.0025 $< E <$ 0.25 V cm$^{-1}$; which mineralizes organics) (Fig. 1) (McIlvride et al., 2003).

Under these conditions, different mechanisms are mainly involved: *i*) electromigration (flow of charged species), *ii*) electroosmosis (flow of pore water and contaminants), *iii*) electrophoresis (colloids' movement) and *iv*) redox reaction on the soil/sediment's particles and/or at the electrodes, prompting the remediation of contaminated sites (Acar et al., 1995; Ferreira et al., 2020; Pamukcu, 2021; Wittle et al., 2009; Zanko et al., 2020). Fig. 2 graphically shows a zoom-area schematic view of the DCTs and the mechanisms treating contaminated sites.

In the case of ECGO, the routes of the involved redox reactions on the soil's particles remain to be clarified. However, it was empirically demonstrated that, using low $E$ values, organics might be desorbed, mobilized and degraded in situ (Fan et al., 2015;

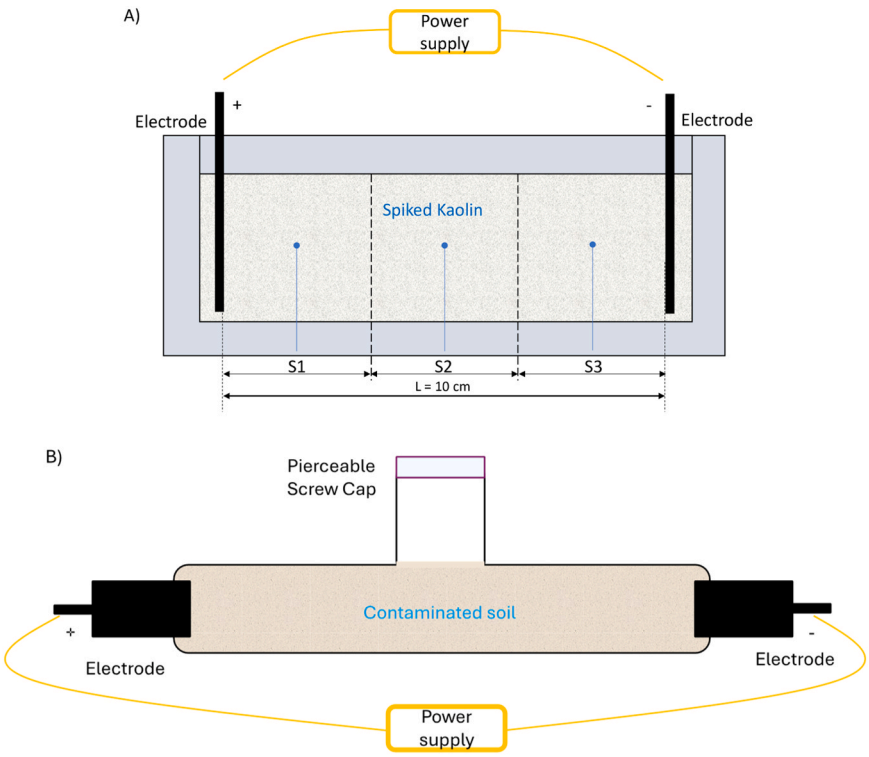


**Fig. 3.** (A) System I: scheme of the electrochemical cell for treating the PhOH spiked kaolin equipped with plate compact graphite electrodes. S1 section is close to the anode, S2 the middle section and S3 section close to the cathode (Proietto et al., 2023). (B) System II: scheme of the gastight electrochemical cell equipped with rod compact graphite electrodes.

Pamukcu, 2021; Proietto et al., 2023, 2024a, 2024b; Saini et al., 2021; Zanko et al., 2020). In particular, ECGO could induce the mineralization of organics (Andreottola and Ferrarese, 2008; Ferreira et al., 2020; Fan et al., 2022) even if no significant proofs were given, up to now, of this possibility. According to Röhrs et al. (2002) and Rahner et al. (2002), wet mineral would perform as a diluted-electrochemical solid-bed reactor and each particle as "micro-conductors". Under the induced *E*, polarized micro-conductors perform as microelectrodes, which might promote redox reaction in the vicinity of the mineral's particle. These give rise to the in situ production of several oxidants and reducing agents (e.g. $HO_2$•, H•, OH•, etc.…) for the organics conversion (near the particles' surface) (Ferrarese and Andreottola, 2007; Pamukcu, 2021; Rahner et al., 2002; Röhrs et al., 2002). In this frame, ECGO is expected to self-generate oxidating and reducing agents (such as H as ion or radical and OH, $HO_2$ and their radicals, respectively) at the electrode sites and within the pores and to give the energy necessary to active chemical reaction. Zanko et al. (2020) studied the ECGO treatment of real sediments from Massachusetts polluted by PCBs, reaching a high reduction in concentration (close to 90 %) after 1900 days. Fan et al. (2015) reported a TPH removal efficiency of approximately 22 % under 0.34 V $cm^{-1}$ after 80 days of electrochemical treatment of a real contaminated soil. Under their operative conditions, the authors highlighted that the recorded reduction in the TPHs concentration can be rationalized in part by the electro-oxidation near the electrodes and in part by the redox reaction on or near the soil's particles (Fan et al., 2015). Saini et al. (2021) reported a reduction of TPHs of 37 % after 7 days under 0.6 V $cm^{-1}$ via ER of soil dredged in Western Australia. Recently, Proietto et al. demonstrated that ECGO technology could be a suitable way to treat clay kaolin or marine sediments for the in-situ removal of phenolic compounds (Proietto et al., 2023), saturated alkanes (Proietto et al., 2024a) or PAHs (Proietto et al., 2024b) using *E* lower than 0.25 V $cm^{-1}$ without the production of secondary effluents and at low energetic consumption. The common findings of these researchers are that the usage of very low *E* values applied by placing electrodes directly into the soils/sediments and without the use of expensive processing fluids can allow simultaneous desorb, transport and also degrade in situ the organic contaminants, regardless of the nature of organics (i.e. PhOH, alkanes, PAHs) and treated soil/sediments (kaolin, clay sand).

However, extra efforts are required to boost the applicative outlook of this tool for the remediation of organics-contaminated soils. Most studies focus on the removal efficiency of one or more target organic contaminants without considering their evolution during the transformation; thus, some of the most burning questions on this topic are: "Which are the byproducts? Are they more harmless than the initial compounds, or are they more toxic pollutants released into the pore water during the process under low *E* values? Can ECGO technology convert organic compounds into $CO_2$ and water?". To our knowledge, no detailed studies exist on this soil/sediment remediation framework under low *E* (i.e. less than 0.25 V $cm^{-1}$). Many studies in the literature have described the transformation of organics under EK conditions using enhancing agents, which must be disposed and treated properly, and relatively high *E* of 1–2 V $cm^{-1}$, which causes high energetic consumption (EC) (Guedes et al., 2019; Maqbool and Jiang 2023; Yuan et al. 2016; Song et al.

2018). However, in these studies, there is no evidence that, in absence of microorganism, organics were mineralized into $CO_2$ in clay (Fan et al., 2022, 2025). If very little knowledge is available for the degradation path of organics in soils and sediments treated by electrochemical methods, the reaction mechanism for the electrochemical oxidation of PhOH and, more generally, of phenolic compounds in water was studied in detail. According to the literature, PhOHs are oxidized first into quinones and/or maleic acid, then to light organics compounds (such as carboxylic acids (CAs)) up to $CO_2$ and water in aqueous electrolyte (Scialdone et al., 2021). In this context, we decided to carry out a systematic work aimed to investigate the effect of ECGO on the transformation of PhOH in many potential byproducts, such as hydroquinone, CAs and $CO_2$ in spiked kaolin using 0.15 V $cm^{-1}$ for 8, 24, 48, 96, 168 and 336 h.

## 2. Materials and methods

### 2.1. Chemicals

PhOH, supplied by Merck (99 % purity CAS 108–95–2), was used as a model hazardous organic pollutant. Bi-distillate water was used as a solvent. Acetonitrile (CAS 75–05–8) and water HPLC grade (CAS 7732–18–5) were purchased from Sigma Aldrich and used for extraction and the analytical apparatus. Compact graphite, supplied by Carlo Erba Reagents, was selected as electrode material.

### 2.2. Electrochemical treatments and spiked-kaolin

Kaolin was selected as a low permeability, low-buffering, reproducible clay mineral model. Kaolin is a hydrate aluminum silicate material ($Al_2Si_2O_5(OH)_4$, CAS 1332–58–7) supplied by Sigma-Aldrich. Kaolin is a fine powder (white/light yellow) with a particle size distribution of 0.1 and 4 $\mu$m when dried (Al-Shahrani and Roberts, 2005). Before being spiked, to remove moisture, kaolin was pretreated by placing 100 g in a Pyrex horizontal vessel in an oven at 105°C for 24 h. Subsequently, kaolin was spiked with PhOH to reach 200 $mg_{PhOH}$ per kg of dried kaolin ($mg_{PhOH}\,kg^{-1}$) and a water content ($W$) of approximately 66 %. More in detail, to obtain 100 g of contaminated kaolin, 60 g of dried kaolin was mixed with 40 mL of 3.2 mM of PhOH water solution. The spiked kaolin was equilibrated using a horizontal shaker (speed rate 200 rpm) for 24 h and a constant temperature of 20°C (Safwat et al., 2019). Prior works stated that the kaolin adsorption capacity of the PhOH is between 300 (Safwat et al., 2019) and 1000 $mg_{PhOH}\,kg^{-1}$ (Acar et al., 1992). At a concentration of PhOH lower than this range, the PhOH removal requires its desorption from the kaolinite into the pore water and its migration towards the electrodes (Acar et al., 1992; Safwat et al., 2019). In the present study, the PhOH initial concentration was fixed at 200 $mg_{PhOH}\,kg^{-1}$, which is less than the saturated sorption content.

The electrochemical cell was previously described in detail by Proietto et al. (2023). Briefly, Fig. 3 reports a schematic view of the homemade Plexiglass® cell with a total empty volume of 60 mL (Fig. 3A) and a scheme of the gastight cell equipped with rod graphite electrode (Fig. 3B). Two compact graphite electrodes of an active area of 3 $cm^2$ were directly inserted into the clay at a distance of 10 cm (Fig. 3A). Contaminated wet kaolin was placed inside the cell by layer, pressed down step by step using a Plexiglass pestle, and vibrated to minimize the void space. 50 g of spiked kaolin was inserted into the cell to be treated (Fig. 3A).

Then, before the electrolysis, a sample of spiked kaolin was taken in duplicate to determine: (*i*) the real initial PhOH concentration ($C^0_{PhOH}$); (*ii*) the pH of the spiked kaolin; and (*iii*) the water content ($W$). This preliminary analysis allowed to avoid the standard deviations due to volatilization of an amount of the charged PhOH and water during the preparation. After preparing the experiment, the cell was sealed with a proper cap in Plexiglass to prevent water evaporation from the sediment bed.

Graphite electrodes were placed in contact with the spiked kaolin (Fig. 3), avoiding any physical barrier and extra electrical resistance. The use of graphite is appealing from an applicative scale since it is eco-friendly, cost-effective, and guarantees good electrical conductivity (Proietto et al., 2023, 2024a).

Electrolyses were performed inducing a constant $E$ of 0.15 V $cm^{-1}$ using an Amel 2549 potentiostat over 8, 24, 48, 96, 168 and 336 h at ambient temperature. Each experiment was carried out in duplicate, and the main results are reported with standard deviations. This allowed to ensure data reproducibility. Preliminary control tests were conducted without the $E$ application.

After each remediation run, portions of treated sediments were collected to determine the residual PhOH concentration, kaolin pH, $W$, CAs, and total organic carbon (TOC) in the pore water. The sampling sections S1, S2 and S3 are represented in Fig. 3. These sections are the sampling positions near the anode, middle and cathode.

### 2.3. Analytical methods

Pure water HPLC grade was used to extract PhOH from the kaolin samples. Approximately 3.0 ± 0.03 g of the well-mixed treated kaolin sample was mixed with 12 g of water HPLC grade (ratio soil:water was 1:4 according to ref. Fan et al. (2025)) in a Teflon-sealed glass vial, *i*) homogenized with a vigorous vortex ARGOlab supplied by GIORGIO BORMAC for 10 min, *ii*) extracted by sonication (FALC ultrasonic bath) for 30 min and *iii*) centrifugated using a centrifuge NEYA 16 at 4500 rpm for 35 min. Then, the supernatant was filtered through 0.22 $\mu$m Nylon membrane and analyzed using TOC and HPLC analysis. Analyses of all samples were performed in duplicate, and the reported results are the averages of the replicates. To ensure that the PhOH as well as other organic byproducts were extracted completely, each kaolin sample was extracted three times.

PhOH and hydroquinone concentrations were estimated using HPLC analysis. An Agilent 1260 fitted with a Kinetex 5 µm C18 column 100 Å 150 * 4.6 mm (Phenomenex) was used. UV detector wavelength was fixed at 214 nm. The mobile phase was water HPLC grade and acetonitrile HPLC grade flowed at 25°C into the column at 1 mL $min^{-1}$. A gradient type of elution was used: *i*) 0 min 20/

80 $\%_{vol/vol}$ acetonitrile/water; *ii*) 5 min 95/5 $\%_{vol/vol}$ acetonitrile/water. Calibrations to determine PhOH and hydroquinone concentrations were built using analytical standards of PhOH (purity > 99 %, Merck, CAS 108–95–2) (retention time (RT) of 3.8 min) and hydroquinone (purity > 99 %, Sigma-Aldrich, CAS 123–31–9) (RT = 1.9 min). CAs were estimated by HPLC Infinity 1260 equipped with a Luna Omega 3μm Polar C18 column (Phenomenex) coupled with a UV detector working at 210 nm. A 100 mM $KH_2PO_4$ aqueous solution (HPLC grade) at pH 2.5 (adjusted $H_3PO_4$) was used as a mobile phase at 1 mL $min^{-1}$ at 25 C°. Calibration curves of the following CAs were performed: oxalic acid (OA, CAS 144–62–7) (RT = 2.67 min); L-(+)-tartaric acid (CAS 87–69–4) (RT = 3.25 min); formic acid (FA, CAS 64–18–6) (RT = 3.55 min); L-(-)-malic acid (CAS 97–67–6) (RT = 4.37 min); acetic acid (CAS 64–19–7) (RT = 5.85 min); maleic acid (MA, CAS 110–16–7) (RT = 7.26 min); citric acid (CAS 77–92–9) (RT = 8.7 min); and, fumaric acid (CAS 110–17–8) (RT = 9.4 min). All CAs have high purity at least of 99 % supplied from Sigma Aldrich. The content of CAs (mg $L^{-1}$) was normalized and obtained as $mg_{i\text{-CAs}}$ per kg of dried kaolin (where *i*- is one of the CAs detected).

The pore water's total organic carbon (TOC) was evaluated by analyzing the surfactant solution using a TOC-L CSH/CSN analyzer Shimadzu. The TOC data in $mg_C\ L^{-1}$ were normalized with respect to the kg of dried kaolin. The initial TOC content in the pore water (TOC°) was approximately 153 ± 5 $mg_C\ kg^{-1}$.

pH in all the sections was measured using a ratio kaolin:water of 1:2.5 with a Checker® pH Tester HANNA® instrument after 6 h of equilibration using a horizontal shaker at 200 rpm. The initial pH of the spiked kaolin was approximately 5.75 ± 0.25.

The water content (*W*), which is namely the moisture of the sediment, was determined according to the NF P 94–050 method following the calculation in (Eq. (1)):

$$W = (w_{evaporated\ water})/w_{dried-sample} = (w_{moist-sample} - w_{dried-sample})/w_{dried-sample} * 100[=]\ \% \quad (1)$$

Where $w_{evaporated\ water}$ is the mass of the evaporated water, instead $w_{moist-sample}$, *and* $w_{dried-sample}$ represent the mass (g) of the wet and dry sample, respectively.

Normalized PhOH concentration was used to evaluate any modification of the PhOH content in the kaolin. This normalized concentration ($C_{PhOH}/C^0_{PhOH}$) is calculated as the ratio of the PhOH concentration at the end of the experiment ($C_{PhOH}$ / $mg_{PhOH}\ kg^{-1}$ of dry kaolin) to the initial concentration ($C^0_{PhOH}$ / $mg_{PhOH}\ kg^{-1}$ of dry kaolin). The $C^0_{PhOH}$ in the kaolin was obtained before starting each electrochemical treatment at zero time by collecting 3.00 ± 0.03 g of spiked kaolin from regions S1, S2 and S3 in Fig. 3 and analyzing them as previously described. The comparison between the values of $C^0_{PhOH}$ in S1, S2 and S3 allowed to check the homogeneous distribution of PhOH along the kaolin inside the cell. In all the cases, the $C^0_{PhOH}$ was approximately to the fixed value of 200 ± 10 $mg_{PhOH}\ kg^{-1}$).

Furthermore, the efficiency of the total PhOH removal ($R_{PhOH}$) was adopted as a figure of merit to evaluate the percentage of residual PhOH in the entire amount of spiked kaolin at the end of each experimental run with respect to its initial content. $R_{PhOH}$ was computed by Eq. (2).

$$R_{PhOH} = (w^0_{PhOH} - w^{kaolin}_{PhOH})/w^0_{PhOH} * 100 = \sum_{n=S1,S2,S3} (1 - C_{PhOH}/C^0_{PhOH})|_n/3) * 100 \quad [=] \quad \% \quad (2)$$

Where $w^0_{PhOH}$ is the initial mass (mg) of PhOH while $w^{kaolin}_{PhOH}$ represents the mass (mg) of PhOH retained by the entire amount of kaolin in the cell at the end of each test.

Energetic consumption (EC) was computed by Eq. (3):

$$EC = \Delta V\ I\ t/w\ [=]\ kWh\ Kg^{-1} \quad (3)$$

where ΔV is the applied cell potential (V), *I* the intensity current (A), t treatment time (s) and *w* is total mass of treated dried kaolin in the experiment (Kg).

To estimate the amount of CAs in each section, it was assumed that the sample analysis refers to each section of approximately 16 g of spiked kaolin at a W of 66 %.

For each test, at least two spiked kaolin samples of 3.00 ± 0.03 g each were taken from S1, S2 and S3 of the cell and analyzed for the quantification of the water content (*W*), pH, PhOH, TOC content and CAs. *W* of the samples was also calculated in the S1, S2 and S3 after the treatment to estimate the residual $C_{PhOH}$ expressed as the amount of PhOH ($mg_{PhOH}$) with respect to the dried kaolin (kg), residual TOC as $mg_C$ per kg of kaolin and CAs content as $mg_{i\text{-CAs}}$ per kg of kaolin, because, under the applied *E* of 0.15 V $cm^{-1}$, it is expected a water movement from the section close to the anode (S1) towards the section close to the cathode (S3) changing the final water content values. All characterization analyses were conducted three times and the main results were reported.

Once each experiment was carried out, the mass balance of the PhOH in the electrochemical cell was checked.

When control tests were performed without inducing an *E*, 93–97 % of the initial PhOH was recuperated.

To detect the $CO_2$ in the gaseous phase an Agilent 7890B Gas Chromatography equipped with Supelco Carboxen® 60/80 column coupled with a TCD detector was used. A GasTight Hamilton syringe was used to inject the gas sample on the GC injector. Gas analysis was carried out selecting the following parameters: i) inlet temperature 120°C, ii) TCD temperature at 275°C, iii) helium (99.999 %, Air Liquide, CAS 7440–59–7) at 30 mL $min^{-1}$ and 1 bar as the carrier gas, iii) column temperature was set at 35°C for 5 min, followed by a 20°C $min^{-1}$ ramp up to 225°C and by an isothermal step at 225°C for 10 min. The retention time of $O_2$ (CAS 7782–44–7), $N_2$ (CAS 7727–37–9) and $CO_2$ (CAS 124–38–9) was 8.7, 9.1 and 18.8 min, respectively.

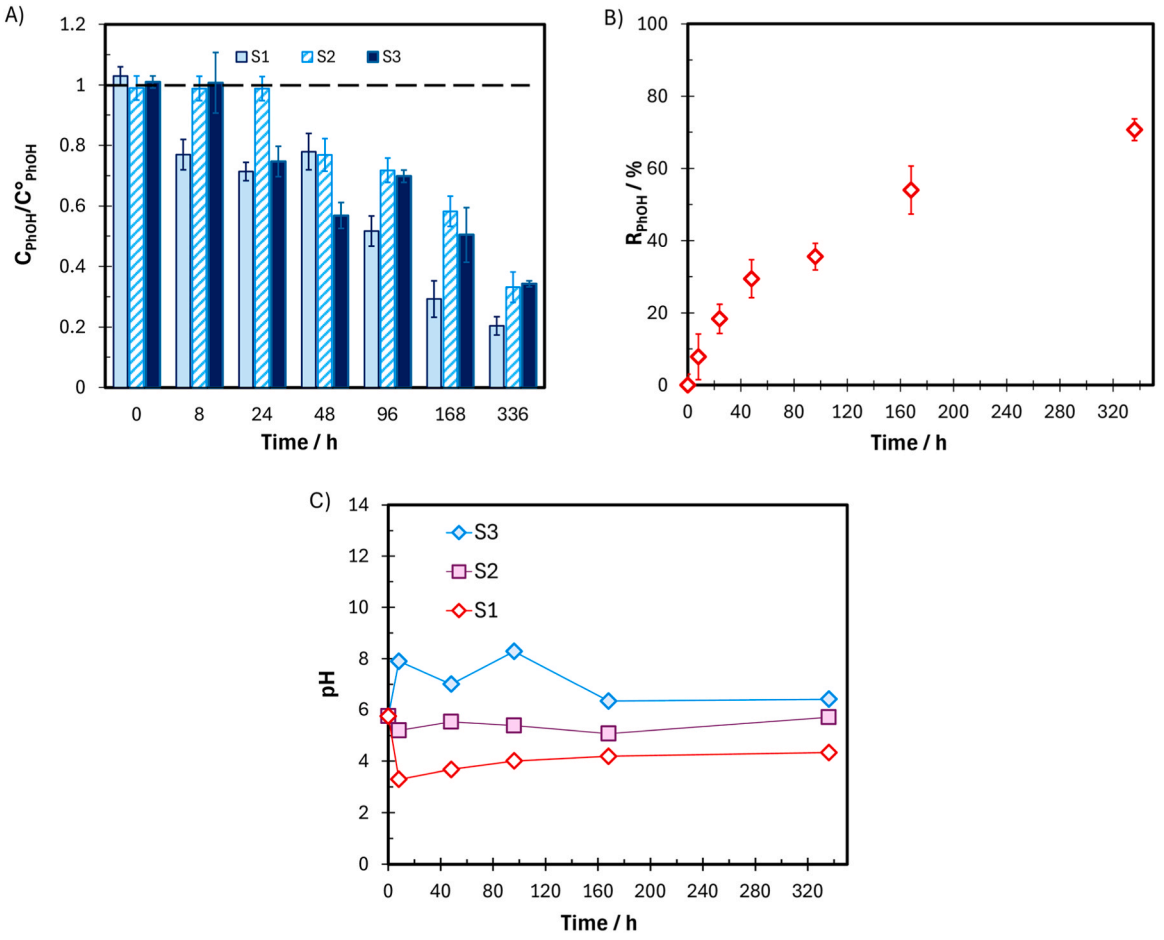


**Fig. 4.** Effect of the time on the electrochemical treatment of kaolin contaminated by PhOH ($C^0_{PhOH}$= 200 mg kg$^{-1}$). (A) Plot of the $C_{PhOH}/C^0_{PhOH}$ in sections S1, S2 and S3, (B) total $R_{PhOH}$ and (C) pH in sections S1, S2 and S3 vs. time. Electrolyses were performed using system I at 0.15 V cm$^{-1}$ for 8, 24, 48, 96, 168 and 336 h. $C_{Phenol}/C^0_{Phenol}$ of 1 indicates the time zero of treatment: black dashed line (— — —).

## 3. Results and discussion

### 3.1. Electrochemical remediation of PhOH-contaminated kaolin under low E value

#### 3.1.1. Effect of the time on PhOH removal

A first series of experiments was planned to study the effect of the treatment time on the electrochemical remediation of PhOH spiked kaolin ($C^0_{PhOH}$ of 200 mg kg$^{-1}$, *W* of 66 %) under very low *E* value of 0.15 V cm$^{-1}$ using compact graphite electrodes. Fig. 4 reports the distribution of $C_{PhOH}/C^0_{PhOH}$ in the sections S1, S2 and S3 of the spiked kaolin (Fig. 4A) and the total removal of PhOH from kaolin ($R_{PhOH}$) (Fig. 4B) at the beginning and after 8, 24, 48, 96, 168 and 336 h of treatment (i.e. 8 h, 1, 2, 4, 7 and 14 days). At the time zero, $C_{PhOH}/C^0_{PhOH}$ were approximately 1 ± 0.05 in sections S1, S2 and S3 (Fig. 4A, $C_{PhOH}/C^0_{PhOH}$ ~ 1 refers to the dashed line), showing that PhOH was homogenously distributed in the cell. In the first stages of the electrochemical treatment, the reduction of the PhOH content took place mainly in the section S1. In contrast, in the second part of the experiments, a relevant removal of PhOH was observed in all the sections. In particular, after 8 h, a slight change in the PhOH distribution was observed; in detail, the $C_{PhOH}/C^0_{PhOH}$ was lower than 1 in the section S1 and close to 1 in the other two sections (Fig. 4A; $C_{PhOH}/C^0_{PhOH}$ was 0.72, 0.99 and 1.01 in S1, S2 and S3, respectively). This change in distribution was coupled with a total $R_{PhOH}$ of approximately 8 % (Fig. 4B).

When the electrochemical treatments were prolonged for 24 h, the distribution of $C_{PhOH}/C^0_{PhOH}$ in the kaolin bed was 0.71, 0.99 and 0.75 in S1, S2 and S3, respectively (Fig. 4A), which was coupled with a slight increase of the total $R_{PhOH}$ to approximately 18 %. In this case, PhOH was accumulated in the middle zone of the cell (section S2). Relevant changes in PhOH distribution were observed when the electrolysis treatment was performed for 48, 96 and 168 h. In all of these cases, the $C_{PhOH}/C^0_{PhOH}$ values were lower than 1 in all the sections (e.g. $C_{PhOH}/C^0_{PhOH}$ was 0.78, 0.77 and 0.57 after 48 h in S1, S2 and S3, respectively, Fig. 4A). In particular, at 96 and 168 h, the $C_{PhOH}/C^0_{PhOH}$ increases by moving from S1 to S2 and S3 ($C_{PhOH}/C^0_{PhOH}$ was 0.52, 0.72 and 0.70 after 96 h and in S1, S2 and S3,

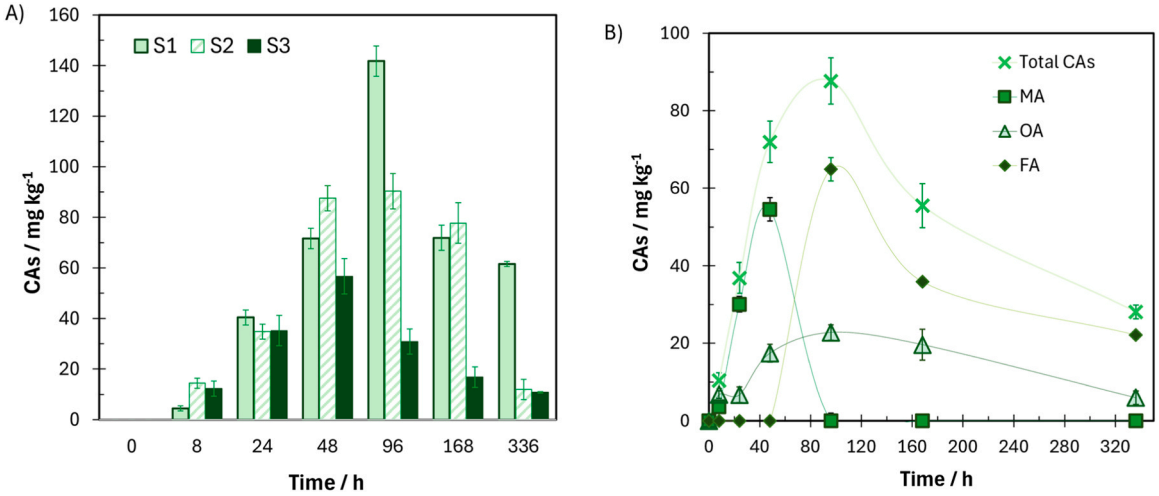


**Fig. 5.** Effect of the time on the CAs (sub-product) obtained during electrochemical treatment of kaolin contaminated by PhOH ($C^0_{PhOH}$= 200 mg $kg^{-1}$). Plot of (A) the distribution of the total CAs in the sections S1, S2 and S3 and (B) MA, OA, FA and the total CAs during the treatment. Electrolyses were performed using system I at 0.15 V $cm^{-1}$ for 8, 24, 48, 96, 168 and 336 h.

respectively, Fig. 4A) reaching a total $R_{PhOH}$ of approximately 36 and 54 % after 96 and 168 h, respectively. A further enhancement of the $R_{PhOH}$ up to 71 % was achieved after 336 h (14 days) (Fig. 4) with a drastic reduction of the PhOH content in all the sections ($C_{PhOH}/C^0_{PhOH}$ was 0.20, 0.33, 0.34 in S1, S2 and S3, respectively). This removal was coupled with a low energetic consumption (EC) of approximately 0.95 $10^{-3}$ kWh $Kg^{-1}$ after 336 h (see Supplementary Material, Figure S1)), which is drastically lower than the one reported in the literature for the EK treating of spiked kaolin of PhOH under 1 V $cm^{-1}$ of approximately 24 $10^{-3}$ kWh $Kg^{-1}$ coupled with similar PhOH removal of approximately 70 % after 96 h (Proietto et al., 2023).

The initial pH of the kaolin was evaluated to be approximately 5.5–6. During the electrolysis, the pH changes: it decreases near the anode (S1) and increases near the cathode (S3) (Fig. 4C). This behaviour is in line with the literature, the change in pH under the adopted conditions is attributed to the electrolysis of pore water that occurs at the electrodes since the applied cell potential is sufficient to activate the water electrolysis (Henrique et al., 2022). Water oxidation produces $H^+$ at the anode, while water reduction generates $OH^-$ at the cathode (Henrique et al., 2022).

These results can be rationalized by taking into account the considerations summarized below.

During the electrochemical treatment of contaminated sites, the wet kaolin is subjected to an induced *E*, which gives rise to the transport of ions, water and contaminants through the low hydraulic permeability mineral due mainly to electroosmosis and electromigration. Hence, these mechanisms might aid the pollutants' transportation (changing the distribution in the bed kaolin) (Reddy and Cameselle, 2009). It worth to note that, although kaolin particles are negatively charged and electrophoretic transport would be possible, according to the literature the migration of charged colloids occurs significantly in soil-liquid mixtures but it is limited for a compact system, like in the our work, since the solid phase is restrained from movement (Fernandez et al., 2009; Yu and Neretnieks, 1996,1997). More in detail, electroosmosis flow moves pore water and contaminants from the anode towards the cathode side. In our case, the electroosmosis flow is expected to be involved, since we observed an accumulation of pore water in section S3 (high W content in S3, see Supplementary Material, Figure S2) and high PhOH concentration nearly the cathode in most of cases (Fig. 4A, section S3). Moreover, electromigration of PhOH was considered not very relevant since, in all the cases, the pH value of kaolin was lower than the pKa of the PhOH (pKa = 9.98); hence, the PhOH cannot be present in dissociated form as phenolic ion.

A total $R_{PhOH}$ higher than zero ($R_{PhOH} > 0$ %), which increases with time, indicates that PhOH conversion into other chemicals takes place in the spiked mineral in addition to the electroosmosis transport. According to the literature, PhOH might be oxidized at both the surface of the anode and near the particle surface due to the in-situ redox reaction by chemical radicals electrogenerated in-situ when a low *E* value is applied to a low permeability kaolin bed (such as hydroxyl radicals (OH·)) (Andreottola and Ferrarese, 2008; Ferrarese and Andreottola, 2007). In addition, in the presence of dissolved oxygen in pore water close to the cathode area (section S3), oxygen is expected to be reduced at the graphite electrode into hydrogen peroxide, an oxidant agent that, according to the literature, aids the conversion of PhOH.

Overall, these findings show that the ER under low *E* value using cheap graphite electrodes in direct contact with the kaolin is a suitable approach to desorb, mobilize and in situ remove PhOH simultaneously; indeed, its removal increases with time up to 70 % after 14 days without adding enhancing agents and under very low *E* values.

### *3.1.2. Investigation of byproducts: carboxylic acids*

The current literature focuses on the removal efficiency of target organic contaminants without considering their evolution during the transformation; however, according to the literature, the oxidation of PhOH in aqueous solutions involves several stages with the formation of quinones and several CAs. Hence, according to these considerations, a series of analyses was performed with the aim to

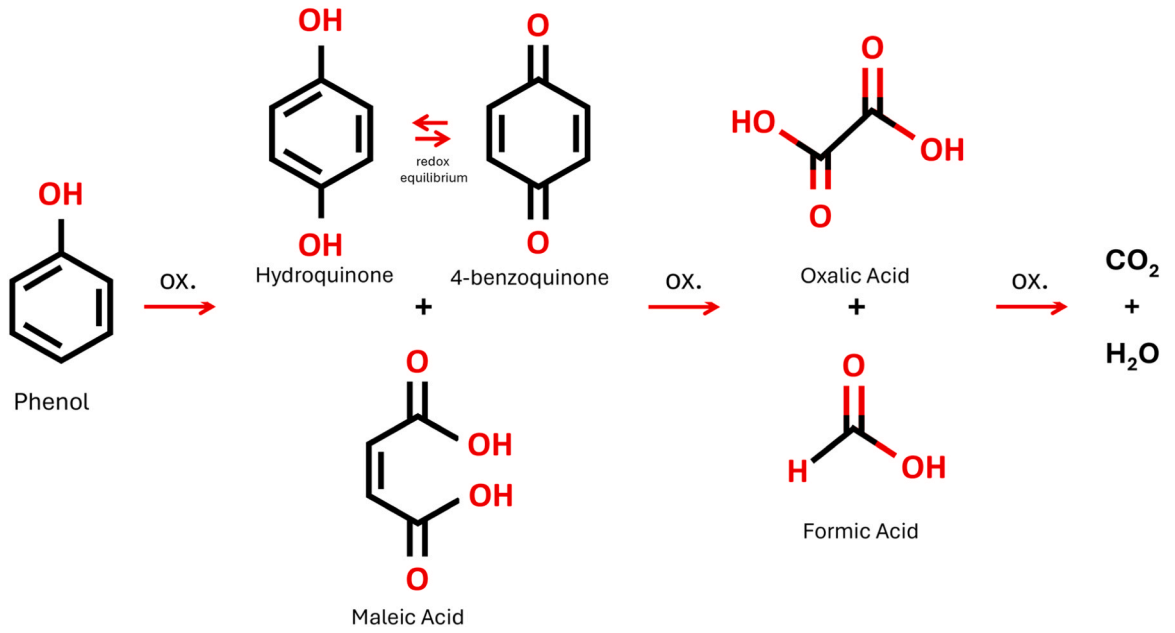


**Fig. 6.** Simplified reaction pathways of the PhOH mineralization in aqueous medium.

check the presence of quinones and CAs. Fig. 5 reports the distribution of the total CAs detected in the spiked kaolin in the sections S1, S2 and S3 (Fig. 5A) and the total amount of CAs in the kaolin (Fig. 5B) during the treatment time. After 8 h, a small amount of CAs was observed in the different sections of treated kaolin (Fig. 5A). When the treatment time was prolonged for 24, 48 and 96 h, a further enhancement of the CAs concentration in each section was observed (Fig. 5A). Overall, the total CAs concentration increases with time reaching a maximum value after 96 h (Fig. 5B). A further increase of the treatment time up to 168 h shows a reduction in each section S1, S2 and S3 of the CAs (Fig. 5A: e.g. 142, 90 and 30 mg $kg^{-1}$ after 96 h vs. 72, 78 and 17 mg $kg^{-1}$ after 168 h in section S1, S2 and S3, respectively) reaching a total CAs of approximately 55 mg $kg^{-1}$ (Fig. 5B). A further enhancement of treatment time up to 336 h shows a reduction in the total CAs concentration (of roughly 28 mg $kg^{-1}$) (Fig. 5B). These results can be attributed to the fact that CAs are simultaneously produced by PhOH oxidation and consumed by their following oxidation: in-situ generation and accumulation of CAs prevail in the first treatment stage when a high concentration of PhOH is present, while CAs content decreases in the second part of the experiments when a low PhOH content is coupled with a relatively high concentration of CAs. Among the CAs investigated, maleic acid (MA), oxalic acid (OA), and formic acid (FA) were the compounds with a higher concentration (Fig. 5B). In particular, the CAs concentrations present a trend with a maximum reached at 48 and 96 h for MA and OA or FA, respectively (Fig. 5B). More in details, a higher content of CAs was generally observed in section S1 (Fig. 5A). This could be attributed to both *i*) the higher oxidation rate occurring at the anode surface and *ii*) the movement of CAs under the influence of the *E*. Based on the pH trends of kaolin during the treatment (Fig. 4C), the detected CAs (MA, FA and OA) are expected to be present predominantly in their anionic forms ($pKa_{FA} = 3.96$; $pKa1_{OA} = 1.25$ $pKa2_{OA} = 4.25$; $pKa1_{MA} = 1.9$; $pKa2_{MA} = 6.2$). Consequently, once formed within the kaolin bed, the anionic species are likely to be transport towards the positive electrode mainly via electromigration, thereby accounting the higher CAs content observed in section S1.

This trend suggests that the reaction mechanism of the PhOH removal in spiked kaolin involves several stages, including first the conversion of PhOH into MA and then its evolution into OA and FA. This behaviour is entirely in line with the reaction mechanism proposed for the degradation of PhOH in aqueous solutions (Devi and Rajashekhar, 2011; Li et al., 2005; Scialdone et al., 2021), which highlights the formation of all the CAs detected (MA, FA and OA). Fig. 6 reports a simplified PhOH degradation pathway often reported in the literature for the electrochemical oxidation of PhOH in water solutions. According to this scheme, PhOH is converted into a miscellaneous of hydroquinone and MA in the early stage of the degradation process, then into OA and FA up to $CO_2$ and water. In this work, hydroquinone was not detected at least within our lower detection limit of approximately 0.05 mg $Kg^{-1}$. Hence, according to all these considerations, it is plausible to affirm that, under the adopted conditions, the main pathway for the PhOH removal from spiked kaolin involves the PhOH aromatic ring is open into MA in the first stage of the treatment and lastly into FA or/and OA (Fig. 6). In this framework, it worth to highlight that the transformation of PhOH into CAs (such as FA and OA) is positive from the environmental point of view, since these compounds have a lower environmental impact. Indeed, the Predicted No-Effect Concentration (PNEC) of the FA is significantly higher than the PhOH one (PNEC: 1.5 mg $Kg^{-1}$ for FA and 0.136 mg $Kg^{-1}$ for PhOH) according to the REACH Regulation ((EC) No. 1907/2006). However, in order to realize a feasible process from an applicative point of view, it would be mandatory to decrease their concentrations in the soil, by a higher conversion in $CO_2$. Hence, in the future, it will be necessary to extend this research to more prolonged and scaled-up systems.

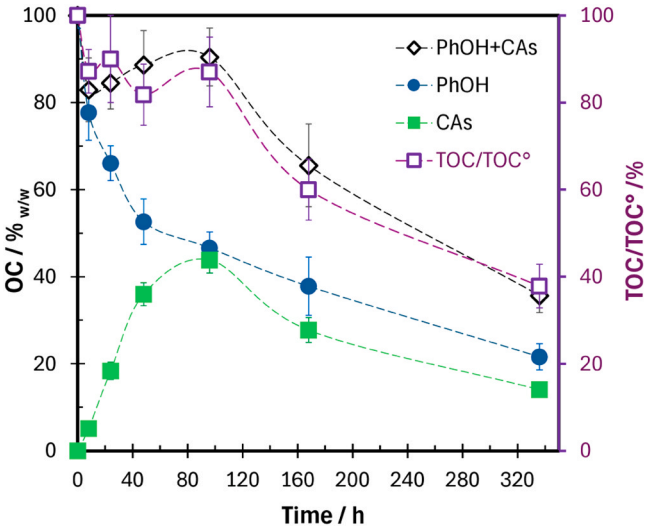


**Fig. 7.** Plot of ratio amount of PhOH, CAs or PhOH+CAs (TotalOC) mass with respect to the initial content of PhOH in mass ($\%_{w/w}$) and the normalized TOC (TOC/TOC°(%)) vs. time as a result of the electrochemical treatment of kaolin contaminated by PhOH ($C^0_{PhOH}$= 200 mg kg$^{-1}$). Electrolyses were performed using system I at 0.15 V cm$^{-1}$ for 8, 24, 48, 96, 168 and 336 h.

### 3.2. Mass balance recovery and total organic carbon

Fig. 7 reports the ratio between the amount of PhOH or CAs and the initial amount of PhOH in terms of mass percentage ($\%_{w/w}$). While the amount of PhOH decreases monotonically over time, reaching approximately 22 % after 336 h, CAs exhibited a curve with a maximum value of approximately 44 % at 96 h (Fig. 7). A noteworthy picture was observed for the ratio between the sum of PhOH and CAs and the initial content of PhOH ($\%_{w/w}$), referred to as TotalOC (Fig. 7) and for the total normalized TOC/TOC° (Fig. 7). The TotalOC presents a quite high value in the initial part of experiments, averaging around 90 ± 8 % up to 96 h of treatment (Fig. 7). However, a further increase of the treatment time up to 168 and 336 h (7 and 14 days, respectively) leads to lower values of TotalOC of approximately 65 ± 9.5 and 40 ± 4 %, respectively (Fig. 7). A similar trend is observed for TOC/TOC° over time. Indeed, the TOC/TOC° value is almost constant and close to an average value of 89 ± 6 % up to 96 h, and decreases significantly in the second part of the experiments giving rise to approximately 60 ± 10 and 38 ± 10 % after 168 and 336 h, respectively, thus showing that an appreciable part of PhOH is converted to $CO_2$ and water and confirming that the reaction scheme reported in Fig. 6 can be applied for the electrochemical treatment of PhOH in soils at low *E*. In particular, it is seen that the data for TotalOC and TOC/TOC° are almost equivalent (Fig. 7), thus showing that PhOH is almost totally converted only in CAs and $CO_2$. In our electrochemical setup, the estimation of $CO_2$ to full close the carbon mass balance is not feasible; therefore, to verify the transformation of PhOH into $CO_2$, an *ad hoc* experiment to treat PhOH spiked kaolin in a gas-tight electrochemical cell (system II, Fig. 3B) was performed under an applied *E* of 0.15 V cm$^{-1}$. In this test, gas-phase samples were collected from headspace of the cell at 0, 24, 48 and 336 h using a gastight syringe through a pierceable septum. To avoid compromising the integrity of the gaseous atmosphere, no PhOH analysis was performed during the treatment. $CO_2$ was detected as early as 24 h, and its concentration continued to increase for all the experiment. It should be noted that these results confirm the conversion into $CO_2$ during the spiked-kaolin treatment under the adopted conditions using the ad-hoc setup (system II), although they do not allow to achieve a full closure of the carbon mass balance for treatment performed with the system I.

## 4. Conclusions

Most studies on soil/sediment electrochemical remediation focus on the removal efficiency of one or more target organic contaminants without considering their transformation and the possible release of other pollutants in the environment. In particular, it was proposed that organics in soils may be potentially mineralized by electrochemical methods, but no experimental evidence was given up to now. In this context, the study aimed to investigate the effect of ECGO on the removal of PhOH and on the generation of many potential byproducts, such as CAs, using cheap graphite electrodes in direct contact with the spiked kaolin at 0.15 V cm$^{-1}$ for 8, 24, 48, 96, 168 and 336 h. Overall, this study confirms that the ECGO under low *E* value is a suitable approach to simultaneously desorb, mobilize and remove in-situ PhOH (up to 70 %). Moreover, the study demonstrates for the first time that several CAs are generated in-situ and that organics can be converted into $CO_2$ and water. More in detail, under the adopted conditions, the main pathway for the PhOH removal from spiked kaolin involves in the first stage of the treatment the opening of the PhOH aromatic ring with the generation of MA, in the second stage its conversion in FA or/and OA and, in the last stages, their mineralization.

Contaminated real soils and sediments present a mixture of contaminants and ions, which can significantly affect the process' performance and the generation of other contaminants' derivates; hence, based on the results reached by this investigation, it will be necessary in future researches to focus on the electroremediation of soils/sediments characterized by the presence of various ions and/

or a mixture of contaminants.

## CRediT authorship contribution statement

**Federica Proietto:** Writing – review & editing, Writing – original draft, Visualization, Methodology, Investigation, Funding acquisition, Data curation, Conceptualization. **Vito Musacchia:** Investigation, Data curation. **Claudia Prestigiacomo:** Investigation, Data curation. **Alessandro Galia:** Writing – review & editing. **Onofrio Scialdone:** Writing – review & editing, Visualization, Supervision.

## Declaration of Competing Interest

The authors declare that they have no known competing financial interests or personal relationships that could have appeared to influence the work reported in this paper.

## Acknowledgements and Funding Information

This study was partially "*Finanziato dall'Unione europea - Next Generation EU", Missione 4, Componente C2 Investimento 1.1* " : Fondo per il Programma Nazionale di Ricerca e Progetti di Rilevante Interesse Nazionale PRIN2022PNRR cod. P2022AK3CA Title "Sustainable rEmedial Approach FoR pOlluted mariNe sedimenTs (SEAFRONT)" CUP B53D23033560001, and from the University of Palermo, which are gratefully acknowledged.

## Appendix A. Supporting information

Supplementary data associated with this article can be found in the online version at doi:10.1016/j.eti.2025.104576.

## Data availability

Data will be made available on request.

## References

Acar, Y.B., Gale, R.J., Alshawabkeh, A.N., Marks, R.E., Puppala, S., Bricka, M., Parker, R., 1995. Electrokinetic remediation: basics and technology status. J. Hazard. Mater. 40, 117–137. https://doi.org/10.1016/0304-3894(94)00066-P.

Acar, Y.B., Li, H., Gale, R.J., 1992. Phenol removal from kaolinite by electrokinetics. J. Geotech. Engrg 118, 1837–1852.

Al-Shahrani, S.S., Roberts, E.P.L., 2005. Electrokinetic removal of caesium from kaolin. J. Hazard Mater. 122, 91–101. https://doi.org/10.1016/j.jhazmat.2005.03.018.

Amato, A., Becci, A., Merli, G., Beolchini, F., Dell`Anno, A., 2026. Environmental sustainability assessment of remediation alternatives for highly contaminated marine sediments. J. Environ. Sci. 159, 731–740. https://doi.org/10.1016/j.jes.2025.04.084.

Andreottola, G., Ferrarese, E., 2008. Application of advanced oxidation processes and electrooxidation for the remediation of river sediments contaminated by PAHs. J. Environ. Sci. Health A. 43, 1361–1372. https://doi.org/10.1080/10934520802231990.

Annamalai, S., Septian, A., Choi, J., Shin, W.S., 2022. Remediation of phenol contaminated soil using persulfate activated by ball-milled colloidal activated carbon. J. Environ. Manag. 310, 114709. https://doi.org/10.1016/j.jenvman.2022.114709.

Barati Fardin, A., Jamshidi-Zanjani, A., 2025. A critical review on soil remediation using electrokinetic-enhanced permeable reactive barriers: challenges and enhancements. Chem. Eng. J. Adv. 23, 100774. https://doi.org/10.1016/j.ceja.2025.100774.

Cui, Y., Yang, C., Qian, G., Huang, J., Zheng, Y., 2006. Remediation of phenol-contaminated sediment by non-uniform electrochemical oxidation reactor. Fresenius. Environ. Bull. 15, 1413–1418.

Devi, L.G., Rajashekhar, K.E., 2011. A kinetic model based on non-linear regression analysis is proposed for the degradation of phenol under UV/solar light using nitrogen doped $TiO_2$. J. Mol. Catal. A Chem. 334, 65–76. https://doi.org/10.1016/j.molcata.2010.10.025.

EU, Soil Strategy for 2023, Communication From The Commission To The European Parliament, The Council, The European Economic And Social Committee And The Committee Of The Regions COM/2021/699 final, ⟨https://eur-lex.europa.eu/legal-content/EN/TXT/?uri=CELEX:52021DC0699⟩.

Fan, R., Guo, S., Li, T., Li, F., Yang, X., Wu, B., 2015. Contributions of electrokinetics and bioremediation in the treatment of different petroleum components. Clean 43, 251–259. https://doi.org/10.1002/clen.201300659.

Fan, R., Tian, H., Wu, Q., Yi, Y., Yan, X., Liu, B., 2022. Mechanism of bio-electrokinetic remediation of pyrene contaminated soil: effects of an electric field on the degradation pathway and microbial metabolic processes. J. Hazard. Mater. 422, 126959. https://doi.org/10.1016/j.jhazmat.2021.126959.

Fan, R., Zhu, M., Yang, B., Yan, X., 2025. Effects of electric field on microbial metabolism in petroleum-polluted soil: insights from microbial function and carbon utilization characteristics. Biochem. Eng. J. 217, 109665. https://doi.org/10.1016/j.bej.2025.109665.

Fernandez, A., Hlavackova, P., Pome`s, V., Sardin, M., 2009. Physico-chemical limitations during the electrokinetic treatment of a polluted soil. Chem. Eng. J. 145, 355–361. https://doi.org/10.1016/j.cej.2008.05.004.

Ferrarese, E., Andreottola, G., 2007. Application of electrochemical techniques for the remediation of soils contaminated with organic pollutants. Association for Environmental Health and Sciences - 23rd Annual International Conference on Soils, Sediments and Water 2007, pp. 343–372 vol. 13.

Ferreira, A.N., Guedes, P., Mateus, E.P., Ribeiro, A.B., Couto, N., 2020. Emerging organic contaminants in soil irrigated with effluent: electrochemical technology as a remediation strategy. Sci. Total Environ. 743, 140544. https://doi.org/10.1016/j.scitotenv.2020.140544.

Gomes, H.I., Dias-Ferreira, C., Ribeiro, A.B., 2013. Overview of in situ and ex situ remediation technologies for PCB-contaminated soils and sediments and obstacles for full-scale application. Sci. Total Environ. 445–446, 237–260. https://doi.org/10.1016/j.scitotenv.2012.11.098.

Guedes, P., Lopes, V., Couto, N., Mateus, E.P., Pereira, C.S., Ribeiro, A.B., 2019. Electrokinetic remediation of contaminants of emergent concern in clay soil: effect of operating parameters. Environ. Pollut. 253, 625–635. https://doi.org/10.1016/j.envpol.2019.07.040.

Henrique, J.M.M., Isidro, J., Saez, C., Dos Santos, V., Rodrigo, E., M.A, 2022. Enhancing electrokinetic soil flushing with air stripping for the treatment of soil polluted with phenol and o-chlorophenol. Electrochim. Acta 432, 141189. https://doi.org/10.1016/j.electacta.2022.141189.
Li, X.Y., Cui, Y.H., Feng, Y.J., Xie, Z.M., Gu, J.D., 2005. Reaction pathways and mechanisms of the electrochemical degradation of phenol on different electrodes. Water Res 39, 1972–1981. https://doi.org/10.1016/j.watres.2005.02.021.
Li, Z., Li, X., 2025. Bibliometric analysis and systematic review on the electrokinetic remediation of contaminated soil and sediment. Environ. Geochem Health 47, 15. https://doi.org/10.1007/s10653-024-02330-7.
Li, X., Wang, X., Weng, L., Zhou, Q., Li, Y., 2017. Microbial fuel cells for Organic-Contaminated soil remedial applications: a review. Energy Technol. 5, 1156–1164. https://doi.org/10.1002/ente.201600674.
Libralato, G., Minetto, D., Lofrano, G., Guida, M., Carotenuto, M., Aliberti, F., Conte, B., Notarnicola, M., 2018. Toxicity assessment within the application of in situ contaminated sediment remediation technologies: a review. Sci. Total Environ. 621, 85–94. https://doi.org/10.1016/j.scitotenv.2017.11.229.
Lofrano, G., Libralato, G., Minetto, D., De Gisi, S., Todaro, F., Conte, B., Calabrò, D., Quatraro, L., Notarnicola, M., 2017. In situ remediation of contaminated marine sediment: an overview. ESPR 24, 5189–5206. https://doi.org/10.1007/s11356-016-8281-x.
Maqbool, T., Jiang, D., 2023. Electrokinetic remediation leads to translocation of dissolved organic matter/nutrients and oxidation of aromatics and polysaccharides. Sci. Total Environ. 876, 162703. https://doi.org/10.1016/j.scitotenv.2023.162703.
McIlvride, W.A., Doering, F., Doering, N., Hill, D.G., Iovenitti, J., 2003. ElectroChemical Remediation Technologies for Metals Remediation in Soil, Sediment and Ground Water, Presentation of Case.
Mouli, P.C., Mohan, S.V., Reddy, S.J., 2004. Electrochemical processes for the remediation of wastewater and contaminated soil: emerging technology. J. Sci. Ind. Res. (India) 63, 11–19.
Ossai, I.C., Ahmed, A., Hassan, A., Hamid, F.S., 2020. Remediation of soil and water contaminated with petroleum hydrocarbon: a review. Environ. Technol. Innov. 17, 100526. https://doi.org/10.1016/j.eti.2019.100526.
Pamukcu, S., 2021. Electrochemical technologies for petroleum contaminated soils. In: Rodrigo, M.A., Dos Santos, E.V. (Eds.), Electrochemically of Contaminated Remediation Assisted Soils, 2021. Springer, pp. 455–484. https://doi.org/10.1007/978-3-030-68140-1_18.
Perelo, L.W., 2010. Review: in situ and bioremediation of organic pollutants in aquatic sediments. J. Hazard Mater. 177, 81–89. https://doi.org/10.1016/j.jhazmat.2009.12.090.
Proietto, F., D'Agostino, F., Bonsignore, M., Del Core, M., Sprovieri, M., Galia, A., Scialdone, O., 2024b. Electrochemical remediation of synthetic and real marine sediments contaminated by PAHs, hg and as under low electric field values. Chemosphere 350, 141009. https://doi.org/10.1016/j.chemosphere.2023.141009.
Proietto, F., Khalil, A., Maouch, W., Galia, A., Scialdone, O., 2023. Electrochemical remediation of phenol contaminated kaolin under low-strength electric fields. Environ. Technol. Innov. 32, 103286. https://doi.org/10.1016/j.eti.2023.103286.
Proietto, F., Meli, P., Prestigiacomo, C., Galia, A., Scialdone, O., 2024a. Study of electrochemical remediation of clay spiked with C12-C18 alkanes. J. Environ. Chem. Eng. 12, 111780. https://doi.org/10.1016/j.jece.2023.111780.
Rahner, D., Ludwig, G., Röhrs, J., 2002. Electrochemically induced reactions in soils - a new approach to the in-situ remediation of contaminated soils? Part 1: the microconductor principle. Electrochim. Acta 47, 1395–1403. https://doi.org/10.1016/S0013-4686(01)00854-4.
Reddy, K.R., Cameselle, C., 2009. Electrochemical Remediation Technologies For Polluted Soils, Sediments And Groundwater. John Wiley & Sons, Inc, Hoboken, New Jersey.
Röhrs, J., Ludwig, G., Rahner, D., 2002. Electrochemically induced reactions in soils - a new approach to the in-situ remediation of contaminated soils? Part 2: remediation experiments with a natural soil containing highly chlorinated hydrocarbons. Electrochim. Acta 47, 1405–1414. https://doi.org/10.1016/S0013-4686(01)00855-6.
Safwat, S.M., Medhat, M., Abdel-Halim, H., 2019. Phenol adsorption onto kaolin and fuller's earth: a comparative study with bentonite. Desalin. Water Treat. 155, 197–206. https://doi.org/10.5004/dwt.2019.24051.
Saini, A., Bekele, D.N., Chadalavada, S., Fang, C., Naidu, R., 2021. Electrokinetic remediation of petroleum hydrocarbon contaminated soil (I). Environ. Technol. Innov. 23, 101585. https://doi.org/10.1016/j.eti.2021.101585.
Scialdone, O., Proietto, F., Galia, A., 2021. Electrochemical production and use of chlorinated oxidants for the treatment of wastewater contaminated by organic pollutants and disinfection. Curr. Opin. Electrochem 27, 100682. https://doi.org/10.1016/j.coelec.2020.100682.
Song, Y., Cang, L., Fang, G., Ata-Ul-Karim, S.T., Xu, H., Zhou, D., 2018. Electrokinetic delivery of anodic in situ generated active chlorine to remediate diesel-contaminated sand. Chem. Eng. J. 337, 499–505. https://doi.org/10.1016/j.cej.2017.12.122.
Thepsithar, P., Roberts, E.P.L., 2006. Removal of phenol from contaminated kaolin using electrokinetically enhanced in situ chemical oxidation. Environ. Sci. Technol. 40, 6098–6103. https://doi.org/10.1021/es060883f.
Wittle, J.K., Pamukcu, S., Bowman, D., Zanko, L.M., Doering, F., 2009. Field studies on sediment remediation. In: Reddy, K.R., Cameselle, C. (Eds.), Electrochemical rEmediation Technologies For Polluted Soils, Sediments And Groundwater, 32. John Wiley & Sons, Inc., Hoboken, New Jersey. https://doi.org/10.1002/9780470523650.ch32.
Yu, J.-W., Neretnieks, I., 1996. Modelling of transport and reaction processes in a porous medium in an electrical field. Chemical Engineering Science 51, 4355-436. https://doi.org/10.1016/S0009-2509(96)00283-7.
Yu, J.-W., Neretnieks, I., 1997. Theoretical evaluation of a technique for electrokinetic decontamination of soils. J. Contam. Hydrol. 26, 291–299. https://doi.org/10.1016/S0169-7722(96)00076-9.
Yuan, Y., Guo, S., Li, F., Wu, B., Yang, X., Li, X., 2016. Coupling electrokinetics with microbial biodegradation enhances the removal of cycloparaffinic hydrocarbons in soils. J. Hazard. Mater. 320, 591–601. https://doi.org/10.1016/j.jhazmat.2016.07.043.
Zanko, L.M., Wittle, J.K., Pamukcu, S., 2020. Case study: electrochemical Geo-Oxidation (ECGO) treatment of massachusetts new bedford harbor sediment PCBs. Electrochim. Acta 354, 136690. https://doi.org/10.1016/j.electacta.2020.136690.